How to cite: *Angew. Chem. Int. Ed.* **2021**, *60*, 11858–11867
International Edition: doi.org/10.1002/anie.202016084
German Edition: doi.org/10.1002/ange.202016084

Cell Communication | Hot Paper

Dynamically Re-Organized Collagen Fiber Bundles Transmit Mechanical Signals and Induce Strongly Correlated Cell Migration and Self-Organization

Qihui Fan, Yu Zheng, Xiaochen Wang, Ruipei Xie, Yu Ding, Boyi Wang, Xiaoyu Yu, Ying Lu, Liyu Liu, Yunliang Li, Ming Li, Yuanjin Zhao, Yang Jiao,* and Fangfu Ye**

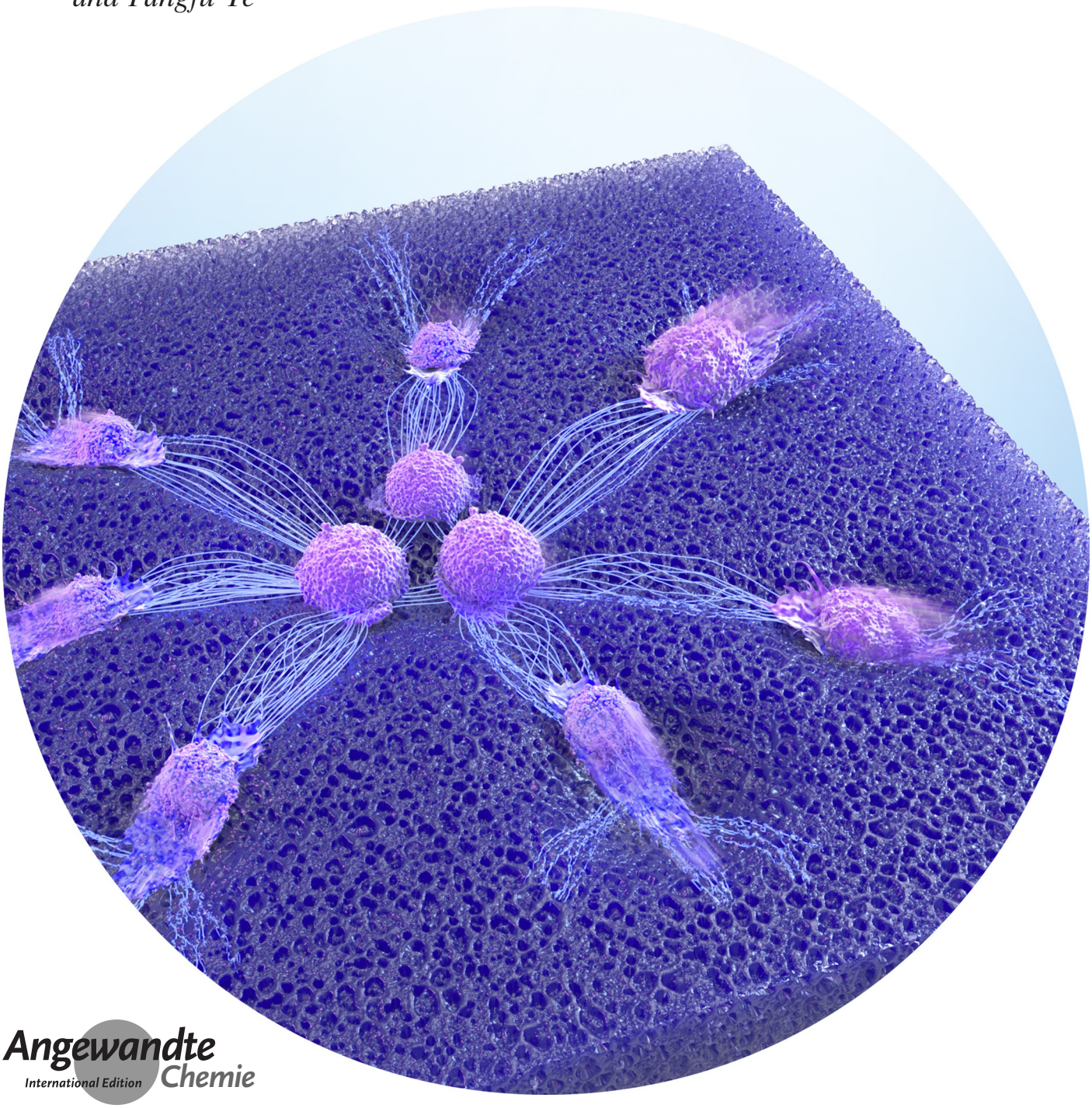

Abstract: *Correlated cell migration in fibrous extracellular matrix (ECM) is important in many biological processes. During migration, cells can remodel the ECM, leading to the formation of mesoscale structures such as fiber bundles. However, how such mesoscale structures regulate correlated single-cells migration remains to be elucidated. Here, using a quasi-3D in vitro model, we investigate how collagen fiber bundles are dynamically re-organized and guide cell migration. By combining laser ablation technique with 3D tracking and active-particle simulations, we definitively show that only the re-organized fiber bundles that carry significant tensile forces can guide strongly correlated cell migration, providing for the first time a direct experimental evidence supporting that matrix-transmitted long-range forces can regulate cell migration and self-organization. This force regulation mechanism can provide new insights for studies on cellular dynamics, fabrication or selection of biomedical materials in tissue repairing, and many other biomedical applications.*

Introduction

Correlated cell migration is crucial to many important physiological and pathological processes such as morphogenesis, wound healing, cancer progression and immune response.[1] The extracellular matrix (ECM) in vivo provides a scaffold for cell migration as well as medium for the propagation of crucial biochemical cues and mechanical signals, as established in recent decades.[2] The microstructure and mechanical properties of the ECM materials can significantly influence cell migration,[3] stem cell differentiation,[1b,4] cancer metastasis,[5] and cardiac cell beating.[1c,6]

How ECM guides cell migration has been extensively studied with various materials and modified micro-structures.[3b,7] During migration, individual cells can generate active pulling forces via actin filament contraction.[8] The forces are applied to ECM via focal adhesion complexes[9] and can deform the ECM.[2d,3b,8,10] It has been reported that cells may migrate along aligned micro-structures of ECM,[3b] a mechanism which is later referred to as contact guidance. Cells can also sense and respond to the local stiffness of their microenvironment via a mechanism called durotaxis,[9] viz., cells usually move towards higher stiffness, although there are some exceptional behaviors depending on cell types. Recently, directed cell migration in response to artificially applied pulling forces on PA-gel has also been observed.[11] However, most of these studies on contact guidance and durotaxis are conducted with artificial materials, such as PA-gel, rather than collagen, which is the most abundant ECM component in vivo and shows specific non-linear viscoelasticity properties and fibrous micro-structures.[1b,12] In addition, numerous simulations have been performed to investigate how the re-organized fiber bundles regulate long-distance cell-cell mechanical communication and collective cell behaviors.[13]

However, to the best of our knowledge, direct experimental evidences are still lacking to verify whether the re-organized collagen fiber bundles between cells indeed carry forces and how they guide cell migration and induce long-range correlation. This is mainly because in the preponderance of the previous experimental studies, either artificial elastic hydrogels were used or cells were entirely embedded within natural hydrogels, hindering cell migration and re-organization of collagen fibers by cells.

Aiming to solve these problems, we constructed a quasi-3D system by utilizing natural fibrous hydrogel collagen with tunable stiffness., with epithelial cells seeded on the interface between the collagen hydrogel and medium, in order to mimick the in vivo microenvironment of epithelial cells. By integrating laser ablation with 3D real-time tracking techniques, we definitively demonstrated that the fiber bundles connecting actively migrating cells are dynamically re-organized by cell contraction, and indeed carry significant tensile forces. The forces transmitted via the fiber bundles lead to strongly correlated cell migration, even at individual-cell level. Once the fiber bundles were cut off by laser, or the cell contraction force was reduced by inhibiting myosin, the strong correlations between migrating cells disappeared. These studies provide direct experimental evidences supporting that re-organized fiber bundles in collagen is critical for

[*] Dr. Q. Fan, Dr. X. Wang, R. Xie, Y. Ding, B. Wang, X. Yu, Prof. Y. Lu, Prof. Y. Li, Prof. M. Li, Prof. F. Ye
Beijing National Laboratory for Condensed Matter Physics and Laboratory of Soft Matter and Biological Physics, Institute of Physics, Chinese Academy of Sciences
Beijing 100190 (China)
E-mail: fye@iphy.ac.cn

Y. Zheng, Prof. Y. Jiao
Department of Physics, Arizona State University
Tempe, AZ 85287 (USA)
E-mail: yang.jiao.2@asu.edu

Dr. X. Wang, Prof. Y. Zhao, Prof. F. Ye
Wenzhou Institute, University of Chinese Academy of Sciences
Wenzhou, Zhejiang 325001 (China)
E-mail: yjzhao@seu.edu.cn

Dr. X. Wang, R. Xie, Y. Ding, B. Wang, X. Yu, Prof. Y. Lu, Prof. M. Li, Prof. F. Ye
School of Physical Sciences, University of Chinese Academy of Sciences
Beijing 100049 (China)

Prof. Y. Lu, Prof. M. Li, Prof. F. Ye
Songshan Lake Materials Laboratory
Dongguan, Guangdong 523808 (China)

Prof. L. Liu
College of Physics, Chongqing University
Chongqing 401331 (China)

Prof. Y. Zhao
Department of Rheumatology and Immunology, The Affiliated Drum Tower Hospital of Nanjing University Medical School
Nanjing 210008 (China)

Prof. Y. Jiao
Materials Science and Engineering, Arizona State University
Tempe, AZ 85287 (USA)

Supporting information and the ORCID identification number(s) for the author(s) of this article can be found under: https://doi.org/10.1002/anie.202016084.

facilitating long-range mechanical communication between migrating cells. Moreover, we investigate how this ECM-mediated force may induce aggregation/organization of cells. We also devised a minimal active-particle model incorporating the mechanism of dynamic-collagen-fibers-mediated mechanical communications, which was able to accurately reproduce the observed collective aggregation behavior. By studying the relationship between the dynamic re-organization of collagen fibers and the correlated behaviors of cells, we obtained results which could lead to a better understanding of important biological processes such as wound healing, cancer metastasis, and embryonic development, and could also assist the design of biomedical materials in these applications.

Results and Discussion

Migration of Epithelial Cells on Thick Collagen Gel Shows Strong Correlation

We carry out cell migration experiments in systems with human mammary gland epithelial cells (MCF-10A-GFP) sparsely distributed on top of 3D extracellular matrix (ECM) based on collagen I hydrogel (i.e., a 800-μm thick layer of collagen gel, see Figure 1a), as well as on top of a 2D solid substrate of Petri dish as control experiments. The advantage of this model system lies in that the fibrous microstructure of collagen gels and their nonlinear mechanical properties are able to support long-range force propagation, as predicted in various numerical studies,[7a,13b,14] and that the strongly motile MCF-10A cells generate significant contractile forces during migration, thus inducing strong cell-ECM mechanical coupling.[8,15] The counterparts of this quasi-3D system also abound in in vivo systems, for example, cells moving on the interface of tissues.

Time-lapse microscopy was applied to record cell migration at 2-min time interval for 8 hours. Figure 1b shows representative trajectories of cells migrating on top of 3D collagen gels and those on solid Petri dish as well. It can be clearly seen that the migration of MCF-10A cells on 3D ECM is manifested to be strongly persistent and even ballistic-like (Supplementary Video 1), which is in contrast to the clear diffusive and random dynamics of MCF-10A cells on 2D solid substrate.

We quantify the single-cell migration dynamics by computing the average migration speed, the mean squared displacement (MSD) $\langle r^2(t)\rangle$, and consider its scaling with time t for the two systems (see Figure 1c), i.e.,

$$\langle r^2(t)\rangle \propto t^{\alpha}, \tag{1}$$

where the exponent α, which can be obtained from the slope of the log-log plot of Equation (1), characterizes the dynamics of the system. For $\alpha = 1$, the dynamic is purely diffusive; and for $\alpha = 2$, the dynamics is purely ballistic. For $1 < \alpha < 2$, the dynamics is super-diffusive, typically representing a mixing of ballistic and diffusive motion (such as persistent random walk).[16] We find that $\alpha = 1.93 \pm 0.06$ for the cell pairs on 3D collagen gel and that $\alpha = 1.28 \pm 0.02$ for the cell pairs on solid Petri dish (Figure 1c). These results clearly indicate the strongly persistent and almost ballistic nature of cell migration on collagen gels within interaction distance, and are consistent with other statistics of the migration dynamics, including directionality and direction autocorrelation, even in large number of cells (Figure S1,S2). The average cell migration speed is also enhanced when cells are approaching each other on collagen (see Figure 1d and Figure S2).

Importantly, we observe strongly correlated migration dynamics for cells on 3D collagens. The typical approaching process is illustrated in Figure 1e by using a representative pair of cells. Specifically, the two separate cells gradually extend the protrusions and rapidly move toward one another, as they sense each other and the distance between the two cells is in an effective "influence range". These strongly correlated pair-migrations are quantified via the normalized cell-pair separation distance as a function of time (Figure 1f), which shows that the distance between a pair of dynamically correlated cells on thick collagen gel rapidly decreases, while the distance between the cells on solid Petri dish substrate randomly fluctuates. This is consistent with the analysis of the correlation between the relative cell velocity $\boldsymbol{v}_r$ and the cell-center displacement vector $\boldsymbol{d}_r$, as quantified by the inner product of the normalized vectors (see Figure 1g), i.e.,

$$\cos\theta = \frac{\mathbf{v}_r \cdot \mathbf{d}_r}{|\mathbf{v}_r||\mathbf{d}_r|} \tag{2}$$

It can be seen that the relative cell velocity and cell-center displacement are strongly aligned in the case of correlated migration of cells on 3D ECM, while these are randomly aligned for cells on the Petri dish.

Re-Organized Fiber Bundles Induce Correlated Cell Migration

To further explore the origin of the observed correlated ballistic-like migration dynamics of MCF-10A cells on quasi-3D collagen gels, we imaged the collagen fibers surrounding randomly selected pairs of cells as they are approaching each other, and analyzed the dynamic re-organization of the collagen fibers via time-lapse laser-scanning confocal microscopy with reflection mode (SP8, Leica). As shown in Figure 2, the collagen fibers in the vicinity of the pulling ends of the migrating cells are re-oriented so that they are locally perpendicular to the pulling edge of the cell. This is mainly due to the contraction of the acto-myosin network of the cell and the resulting active tensile (pulling) forces, which are applied to the ECM network via cell focal adhesion complexes.[14a] Interestingly, for a pair of migrating cells approaching each other, the collagen fibers in the region between the two cells are significantly re-organized (i.e., remodeled) to form thick and long fiber bundles that are parallel to the line connecting the cell centers (see Figure 2a and Supplementary Video 2). The "bridged" cells continue to migrate towards one another along the "bridge" of fiber bundles connecting them.

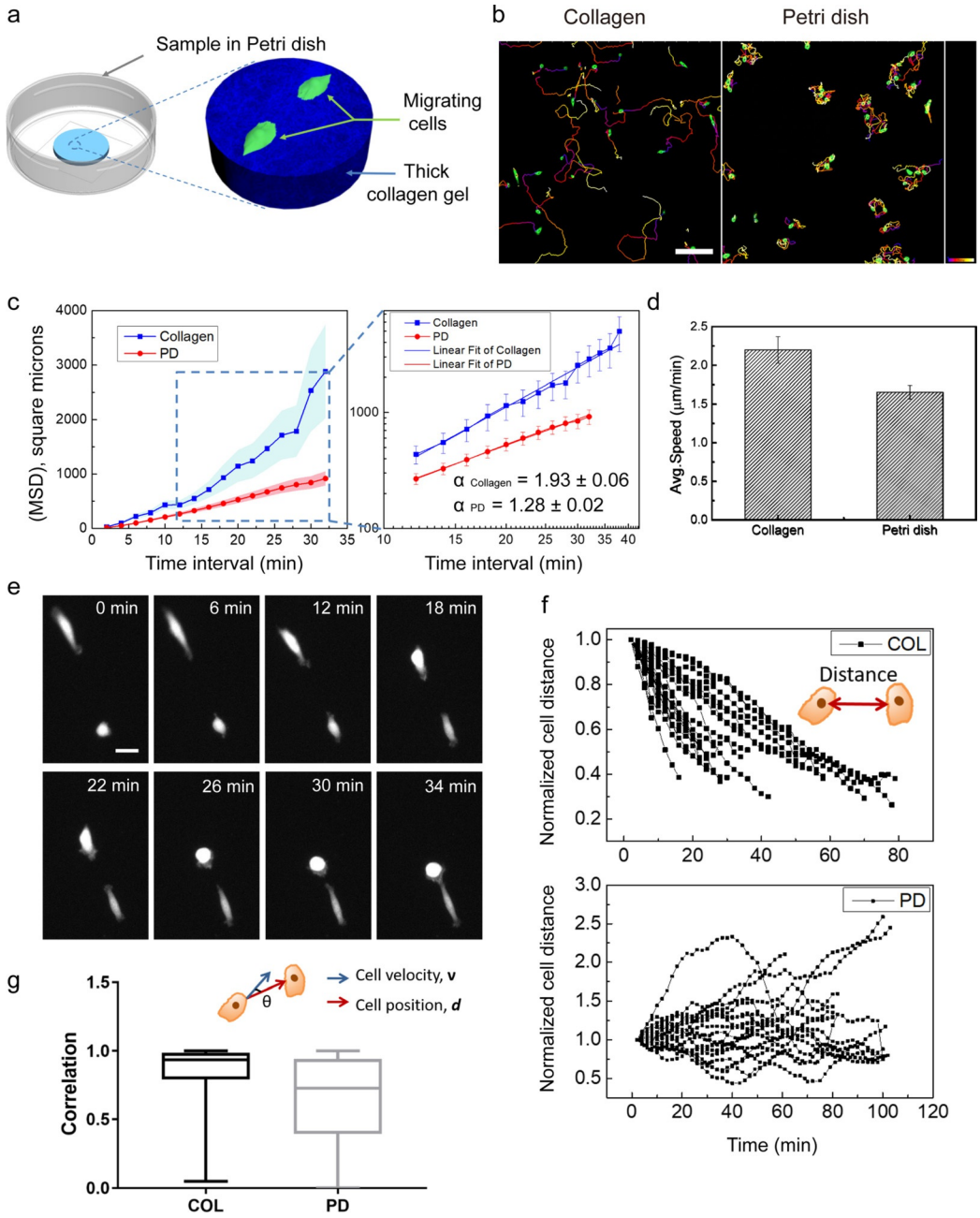

Figure 1. MCF-10A cells migrating on thick (3D) collagen gel exhibit anisotropic persistent random walk behaviors with strong correlation. a) Schematic illustration of the experimental system. b) Representative cell trajectories show the persistent migration (on thick collagen gel) and random migration (on Petri dish). Scale bar is 300 μm. c) Mean square displacement (MSD) analysis for the persistent migration on 3D collagen gel and random migration on Petri dish (PD) for cell-pairs within correlated distance. Data are presented as mean ± s.e.m, $n = 107$ for collagen group and $n = 105$ for PD group. The inset shows the linear fitting of the log-log plot of MSD v.s. time, with the value α (the slope in the log-log plot) quantifying the modes of migration dynamics. d) Average cell migration speeds for the persistent migration on collagen gel and random migration on Petri dish for cell-pairs within correlated distance. e) Images of a typical pair of MCF-10A cells migrating on collagen gel. Scale bar is 30 μm. f) Statistics of normalized relative distance between cell pairs on collagen gel and solid Petri dish. g) Statistics of the correlation of relative cell velocity and cell-center displacement vector.

In addition, the time-lapse analysis indicates that the re-organization of the collagen fibers is not permanent (Figure 2a, orange arrow indicated position). For example, once the direction of cell motion changes, the re-organized fiber bundles originally near its pulling edge also disappear. This suggests that the re-organization is mainly mechanical in nature, due to the elastic deformation and re-orientation of the collagen fibers caused by the active pulling of migrating cells (Figure S6).

This mechanism is supported by our simulations (see Figure 2c and d), in which cells are modeled as contractile spheres whose surfaces are attached to fibers of discrete bond-node model of ECM network with non-linear mechanical properties (see Ref. [14a] and Methods in Supporting

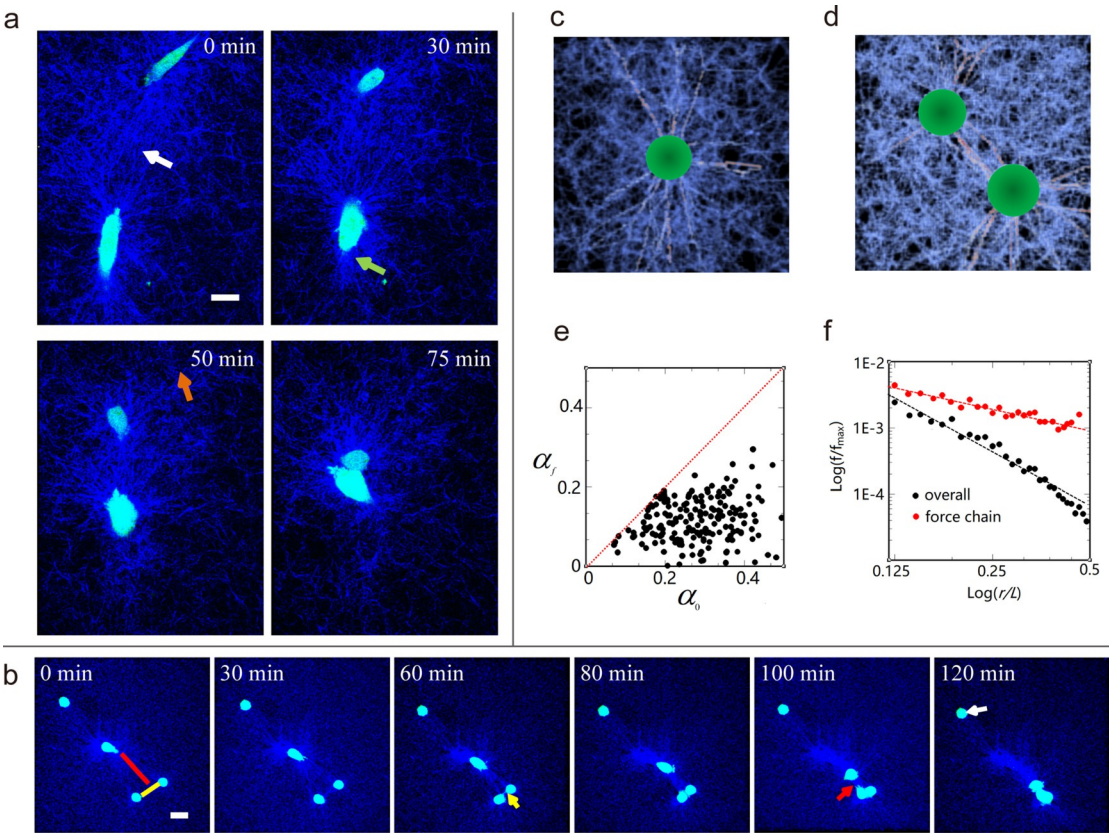

Figure 2. Strongly correlated cell migration mediated by re-organized fiber bundles. a) A representative pair of cells (green) exhibiting strongly correlated migrating dynamics and the remodeled collagen fiber bundles (blue). The white arrow indicates the long fiber-bundle bridge between the cells, and the green arrow points at the short fiber bundles locally perpendicular to the pulling edge of the cell but not connecting to other cells. The orange arrow shows the area where temporally remodeled densified collagen fiber bundles were released and short fibers were restored. b) A representative multi-cell network showing typical multi-cell migration dynamics. The yellow marking line links two cells that are closer to each other than the red-line marked cell. The yellow-line marked cells approached each other much faster. The white arrow marked cell kept the round shape and didn't re-organize the surrounding collagen, thus it didn't communicate with other cells via fiber-mediated force transmission nor exhibited any significant migration. c) and d) respectively shows the remodeling of collagen fibers by the active pulling forces generated by a single isotropic contractile cell and a pair of contractile cells. The fibers carrying large forces (i.e., larger than 10% of the maximal tensile force), which form linear chain-like structures (i.e., force chains), are highlighted in red. e) Scatter plots of the acute angle between two successive fiber segments along the force chains before (α_0) and after (α_f) cell contraction. The scatter distribution clearly shows that the pulling forces due to cell contraction lead to better alignment of the fibers. f) Fiber-mediated long-range force transmission. The force on the fiber bundles decays much slower with a scaling $\approx 1/r^{\beta}$ (with $\beta \approx 0.68$) than in a continuous elastic medium (with $\approx 1/r$). All scale bars (in white) are 30 μm.

Information for details). In particular, as the cell contracts isotopically, the fibers attached to the cell surface are pulled towards the cell center. The pulling forces result in re-orientation and alignment of successive fiber segments to form linear chain-like structures (see Figure 2e), whose extent ($\approx$20 to 40 μm) is much larger than the average length of the fiber segment ($\approx$2 to 5 μm),[14a,b,17] representing the experimentally observed fiber bundles. It is found that such chain-like structures (i.e., fiber bundles) carry the majority of the tensile forces generated by the cell, and the force on the fiber bundles decays much slower, with a scaling $\approx 1/r^{\beta}$ (with $\beta \approx 0.68$), than that in a continuous elastic medium (with $\approx 1/r$) (see Figure 2f).[14a]

In a multi-cell system, similar correlations between the re-organized fiber-bundle network and collective migration dynamics are observed. In particular, the migrating cells re-organize the surrounding collagen fibers, forming multiple "bridges" connecting their neighbors, as shown in Figure 2b (Supplementary video 3). The cell pairs with smaller separation distances usually exhibit stronger correlated dynamics, and move more rapidly toward each other. Other cells in relatively large distances to the "attracting" cell pairs can also migrate toward them following the fiber-bundle "bridges". Cells that are not active, i.e., non-contracting, cannot re-organize the local ECM to form fiber bundles, and thus, are not able to form bridges with other cells nor migrate (Figure 2b, white arrow). For example, cells undergoing mitosis usually assume a round shape and do not generate strong contraction nor communicate with other near-by cells.

Similar ECM remodeling and collective migration dynamics are also observed in epithelial cells MDCK. Although MDCK cells migrate very slowly, the bridge-like fiber bundles due to ECM remodeling can still be clearly observed, and they also guide collective cell-clusters migration (see Figure S8). These results indicate that the underlying mechanism

associated with the regulation of collective migration dynamics via re-organized fiber-bundles might be generic for adherent cells.

Re-Organized Fiber Bundles Carry Significant Tensile Forces

An important implication of our simulations is that the re-organized fiber bundles carry the majority of the active tensile forces generated by cell contraction, which are transmitted via the fiber bundles to distant cells. This suggests a novel mechanism based on fiber-mediated long-range force transmission for mechanical signaling among migrating cells, which could lead to a rich spectrum of collective behaviors.

In order to experimentally verify this simulation prediction, we employed laser ablation technique (Leica, LMD7000) to cut off the fiber bundles between the strongly correlated cells, and then used laser scanning confocal microscope system for 3D imaging and tracking. We observed that after the cut-off the incision was pulled open rapidly (in less than a minute after the cutting), due to the pre-stored strain energy (and thus, forces) in the re-organized fiber bundles induced by the active cell contraction. In the subsequent 3 to 4 min, the incision continued to open up gradually due to the pulling force applied by the cells and transmitted via the fiber bundles on each side of the incision (Figure 3a; Supplementary video 4).

Assuming the system remained in the elastic regime, we then utilized the information on the initial opening of the cut to estimate the magnitude of the cellular pulling forces. As shown in Figure 3c, we model the cells as a pair of spheres with contractile boundaries embedded in the ECM (modeled as a continuum, see Methods in Supporting Information for details), with a thin cut in the middle region between the two cells. The isotropic contraction of the cells pulls open the cut. By matching the simulated width of the open cut with the experiment data in the first minute after cutting, we are able to inversely derive the required contraction boundary conditions and the associated pulling force, as well as the stress/strain distribution in the ECM. Using this model, the pulling force is estimated as ≈ 20 nN.

In our control experiment, in which the cut position was in a collagen region without re-orientated fiber bundles, the incision did not open up and remained the original shape and

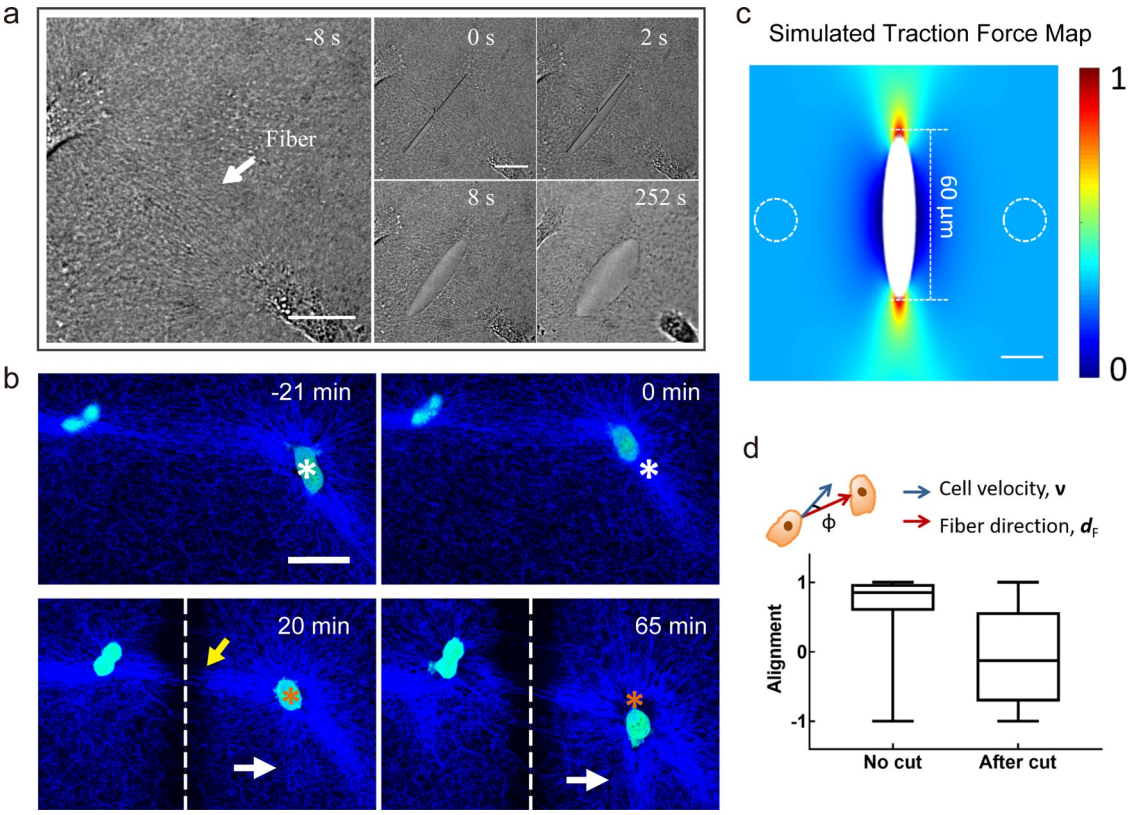

Figure 3. Stressed fiber bundles direct cell migration. a) shows rapid opening of laser-cut incision. b) shows the change of cell trajectories resulting from laser ablation: before the ablation, cells migrate toward each other (white star marking the original cell position before laser ablation); after the fiber-bundle "bridge" was cut off by laser ablation (dash line), the cells stopped migrating along the bundle direction and gradually change their migration directions (orange star marking the original cell position after laser ablation) by forming new fiber bundles (white arrow) in 10–50 min, even though the previous fiber bundles still exist (yellow arrow). c) Simulation results of the cell traction force field (normalized with respect to the maximal traction force) near the laser cut. Dashed circles mark the cells position. d) Correlation between the relative cell migration velocity and the fiber-bundle direction between cell pair, which is defined as "Alignment", corresponding to the $\cos\phi$ in Equation (3). Data are presented as mean $\pm$ s.e.m, $n=80$ for "No cut" group and $n=104$ for "After cut" group in three parallel samples for each group. It can be clearly seen that the cell migration is strongly correlated with the fiber bundle direction before cutting; after the bundles were cut, the cell migration is uncorrelated with the original bundle direction.

size after the cutting (Figure S9a). Similar results were obtained in the myosin inhibited cell samples and 4% paraformaldyhide (PFA) fixed cell samples (Figure S9b,c). These results clearly indicate that the fiber bundles, formed due to elastic remodeling of the ECM by the contractile cells, transmit active tensile forces as mechanical signals among migrating cells.

Furthermore, once the fiber bundles were cut off, the cells did not continue to migrate along the original fiber bundle direction. Instead they changed their migration direction and gradually induced new oriented fiber bundles (within 10–50 min after cutting) (Figure 3b). This process is also quantified by monitoring the correlation between the relative cell migration velocity $\boldsymbol{v}_r$ and the fiber-bundle direction between cell pair $\boldsymbol{d}_F$ (see Figure 3d), i.e.,

$$\cos\phi = \frac{\mathbf{v}_r \cdot \mathbf{d}_F}{|\mathbf{v}_r||\mathbf{d}_F|}. \tag{3}$$

It can be clearly seen from Figure 3d that the cell migration is strongly correlated with the fiber bundle direction before the cutting. After the bundles were cut, the cell migration is largely uncorrelated with the original bundle direction. In addition, it is commonly observed that the cells would eventually migrate to other nearby cells via newly emerged re-organized fiber bundles (Figure 3b), or to the tip of the incision (newly formed stressed point) if the tip is close to the cell (Figure S10). These results clearly indicate that cells respond to the forces transmitted by the re-organized fiber bundles.

In order to exclude the interference from the chemical signals on the migration correlation, a negative control test was conducted, in which a continuous gas flow was injected into the medium to disturb the diffusion of chemical factors. We found that the cells in the negative control test still exhibit strongly correlated migration dynamics, which confirms that fiber-mediated force transmission plays a key role in giving rise to the observed migration dynamics (Figure S11).

We note that the aforementioned results provide the first direct experimental evidence supporting that re-organized fiber bundles transmit active forces and induce strongly correlated migration of adherent cells. Furthermore, it can be clearly seen from our laser ablation experiments that the cut fiber bundles, although having highly aligned individual fibers, do not carry active forces and are thus not able to influence cell migration (Figure 3d). The mechanism reported in our work is therefore distinctly different from the well-established contact guidance mechanism.

Reducing Cell Contraction Force Decreases Mechanical Communication Between Cells

To further explore the force transmission mechanism, we applied myosin inhibitor, Blebbistatin, to reduce cell contraction force on the ECM, and examined how the re-organization of collagen fiber bundles and the expression of paxillin and actin (two important proteins related to cell motility, the former of which is one component of cell's focal adhesion) are influenced. The results show clearly that when the cell contraction force was reduced, there was almost no collagen fiber bundles formed among migrating cells (Figure 4d); meanwhile, the expressions of paxillin and actin also decreased, as semi-quantified from immunofluorescent results (Figure 4c). However, the paxillin expression of cells on solid substrate was not affected by Blebbistatin's inhibiting myosin.[18] It is also worthy to notice that with the presence of collagen the paxillin distributes more diffusely through the whole cells, without many plaque-like focal adhesions in the protrusion of cells like the case on solid substrate (Figure 4d), because the complex micro-structure and mechanical signals of the collagen substrate require dynamic and transient response of paxillin. The actin expression shows that the cells' protrusions are flat lamellipodia on solid substrate and tip-like filopodia on collagen, because without the mechanical signal to guide the migration the flat spreading lamellipodia enable the cells on solid substrate to search for more area.

We proceed to investigate how the correlation of cell migration is influenced by the inhibition of myosin. We define the velocity correlation function (S value) to quantify the correlation during the process of cell-pair's approaching each other (Supplementary Eq. 4). Due to the strong correlation, the S value of migrating cells (in effective range) on collagen is much higher than that of cells on solid Petri dish substrate (Figure 4a). However, once the cell contraction force was reduced by inhibiting myosin with Blebbistatin, the S value of cells on collagen decreased dramatically, to a level similar to that of cells on Petri dish (Figure 4a), because of the loss of mechanical signals among cells. Meanwhile, the cell's speed also decreased if contraction force was reduced (Figure 4b). These results show clearly that the mechanical signaling induced by the cell contraction and transmitted by the fiber bundles plays a key role in inducing the migration correlation of cells.

Long-Range Force Transmission Induces Cellular Self-Assembly

After verifying the mechanism that remodeled fiber bundles transmit active cellular forces which in turn regulate cell migration, we now investigate the collective migration dynamics emerging from this mechanism. To this end, we first devise a computational model which generalizes the active particle with polarized attraction (APPA) model[19] by imposing an additional polarized effective cell-cell attractive force $\boldsymbol{f}_a \approx 1/r^{\alpha}$, where r is the separation distance between two cell centers and $0 < \alpha \leq 1$ characterizes the propagation of the active force and depends on the microstructure and mechanical properties of the ECM. Importantly, $\boldsymbol{f}_a$ is "turned on" only when the polarization (i.e., migrating) direction of a pair of cells is anti-parallel, i.e., the cells are migrating towards each other. This corresponds to the case that two cells migrating toward each other (with anti-parallel velocities) collectively remodel the ECM in between to generate fiber bundles for force transmission. The details of this model are provided in the Methods of Supporting Information.

Using this generalized APPA model, we investigate the collective migration behaviors of MCF-10A cells on 3D ECM

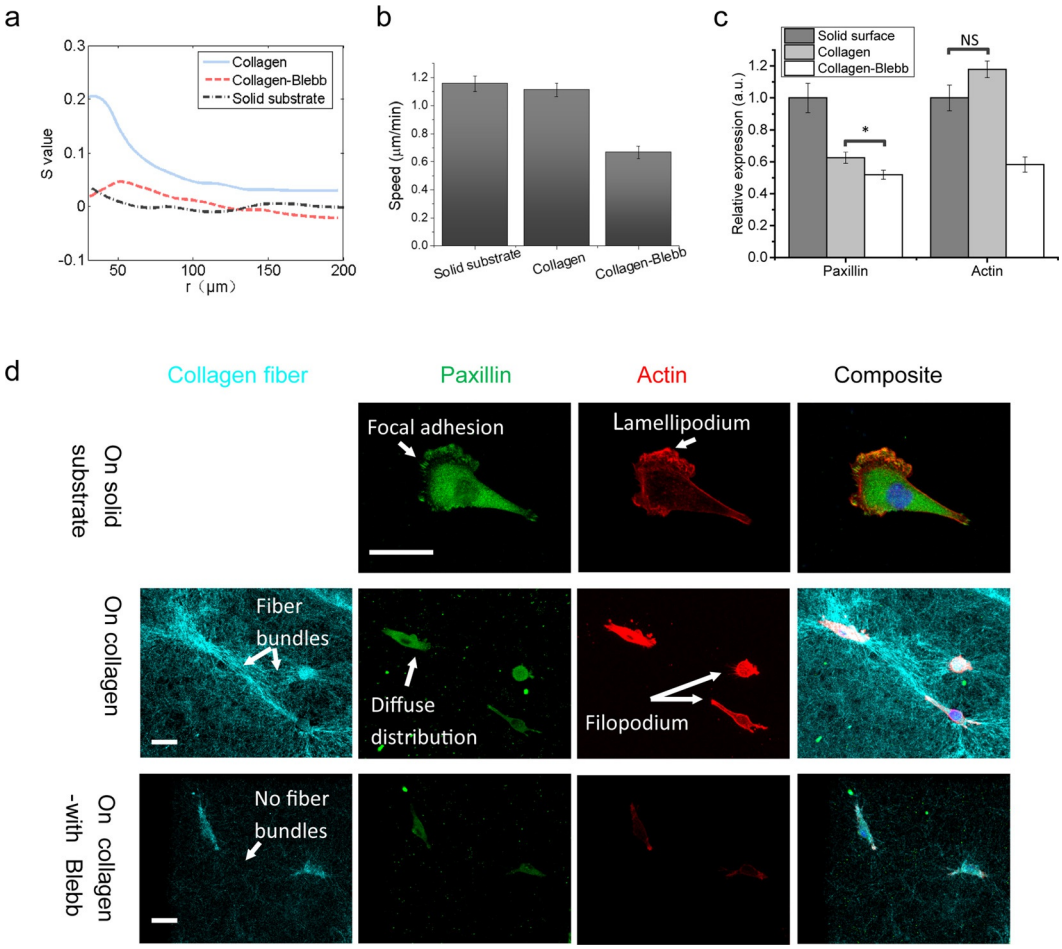

Figure 4. Protein examination of normal cells on solid substrate, normal cells on collagen, and Blebbistatin-treated cells on collagen. a) Velocity correlation (S value), b) speed, and c) relative protein expression of cells on solid substrates, cells on collagen, and Blebbistatin-treated cells on collagen [one-way ANOVA, * $P<0.05$, NS (not significant)]. d) Representative images of collagen fiber, paxillin, and actin expression of cells on solid substrate, cells on collagen, and Blebbistatin-treated cells on collagen, where the composite column corresponds to the superposition of all the other columns. All scale bars are 30 μm.

with two distinct cell densities (defined as the number of cells per unit area within a domain of observation): $\rho = 10^{-4}$ and 5×10^{-4} μm^{-2}, respectively. We also define a characteristic near-neighbor distance $l_n = \rho^{-1/2}$. At the low density (i.e., $l_n \approx 100$ μm), the cells remain separated and their migrations are un-correlated, as can be seen, respectively from the cluster statistics and the velocity correlation function (see Supplementary Eq. 4 for definition) shown in Figure 5e and f. In particular, we compute the normalized size of the dominant (i.e., largest) cluster, which is defined as the number of cells in this cluster over the total number of cells in the system. At the high density (i.e., $l_n \approx 48$ μm), the cells rapidly aggregate from an initial uniform distribution into a dominant compact cluster (see Figure 5e). Importantly, the velocities of the cells are strongly correlated, as manifested by the slow linear decrease of the velocity correlation function (see Figure 5f). To further understand the origin of the strong velocity correlation, we plot the instantaneous velocity map (see Figure 5a,b), which clearly shows that the velocities of the cells within the dominant cluster all tend to point to the center of the cluster. Although it is well known that activity alone (i.e., active Brownian particles without the polarized effective attractive interactions) can also lead to aggregation behavior at high densities, the particles in the aggregated cluster in such cases do not exhibit any significant velocity correlations (see SI for details).

The model predictions are subsequently verified in our experiments. In particular, we randomly distribute the MCF-10A cells in a round pattern of ≈1 mm-diameter on collagen-based ECM with two distinct cell densities, corresponding to the simulation values (i.e., $\approx 10^{-4}$ and 5×10^{-4} μm^{-2}). Similar to the simulation results, rapid and strong aggregation was observed in the high-density system while the cells in the low-density system remain separated (see Figure 5c). We also computed the cluster statistics (Figure 5e) and the velocity correlation functions (see Figure 5f). Consistent with the simulation results, the cells within the cluster in the high-density system exhibit strong dynamic correlations, as indicated by the long-range linearly-decreasing velocity correlation function, and strong centripetal migration dynamics, as shown by the cell trajectories (Figure 5c,d, and Supplementary Video 5). The cells in the low-density system are largely uncorrelated, as evidenced by the flat low-value (≈ 0) velocity correlation function and the random cell trajectories.

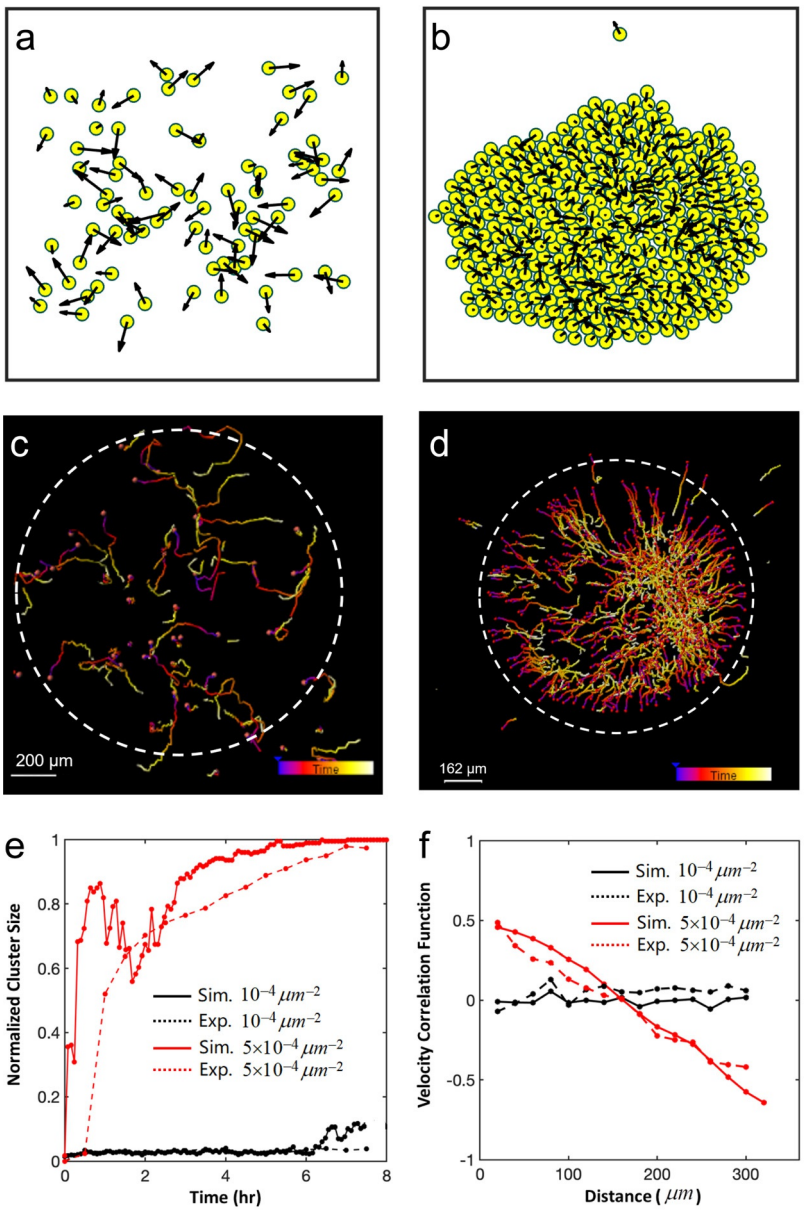

Figure 5. ECM-mediated long-range mechanical coupling leads to strong centripetal migration dynamics and aggregation of MCF-10A cells. a) and b) respectively shows snapshots of velocity distribution in simulated cell systems at two cell densities $\rho = 10^{-4}$ and 5×10^{-4} μm^{-2}. The arrows (positioned at the centers of the cells which are represented as circles) indicate the cell velocities. c) and d) respectively shows the cell trajectories for around 6 hours in the experimental systems (MCF-10A cells on 3D collagen gel) at two cell densities $\rho = 10^{-4}$ and 5×10^{-4} μm^{-2}. The color of trajectories is from purple to yellow, representing the time lapse. Round points represent the initial cell positions. The centripetal migration mode at the high cell density can be clearly seen. e) shows the evolution of the cluster statistics as a function of time for both the simulated and experimental systems, which clearly indicates aggregation behavior at high cellular density in both systems. f) shows the velocity correlation functions for both the simulated and experimental systems.

In the control experiment, the MCF-10A cells were randomly distributed on solid substrate of Petri dish with $\rho \approx 5\times10^{-4}$ μm^{-2}, and no significant collective dynamics is observed (see Figure S12e).

Both our simulations and experiments clearly indicate that the ECM-mediated mechanical coupling between migrating cells breaks the symmetry of random cellular motion and leads to cell aggregation as well as strongly correlated centripetal migration dynamics. The latter is not observed in multi-cellular systems without ECM-mediated mechanical coupling, and is thus a unique consequence of this novel mechanism.

Conclusion

Through a synergy of experimental and computational efforts, we have elucidated the mechanism underlying long-range mechanical coupling of migrating cells. In particular, we show by using laser ablation techniques that the fiber bundles formed due to mechanical remodeling of ECM by migrating cells carry significant tensile forces and thus facilitate long-range force propagation in ECM. Moreover, we show that these forces can regulate cell migration dynamics and induce strong correlation, leading to cell aggregation and unique centripetal migration at high cellular densities.

We emphasize that the long-range dynamic force reported here is the force transmitted through the collagen fiber bundles in natural ECM between individual cells, rather than that relaying through cell-cell junctions as reported in previous studies on cell monolayers. This remotely transmitted force can induce cell-cell communication without cells' contact. Although such long-range force has recently been reported to regulate myofibroblast-fibroblast interaction[20] and collective cancer cells invasion,[21] a direct verification of the role of fiber bundles in such regulation is still lacking. Owing to the proper choice of quasi-3D models, which can provide natural fibrous hydrogel as ECM for transmitting force, on one hand, and avoid encapsulating cells and restricting their motility, on the other hand, we were able to quantify the correlation of cell dynamics and the structure change of fiber bundles, and therefore provide a direct experimental evidence on how fiber bundles participate in such long range regulation at single-cell level. These results may open a new window for studies on cellular dynamics in tissue repair and other important biological processes.

Data Availability Statement

All data needed to evaluate the conclusions in the paper are present in the paper and/or the Supplementary Materials.

Additional data related to this paper may be requested from the authors.

Acknowledgements

We thank T. C. Lubensky, D. A. Weitz, H. Chate, M. Turner, R. Podgornik, and J. Tang for helpful discussions, and Y. Zhai for assisting with apparatus. This research was supported by the National Key Research and Development Program of China (2020YFA0908200), the National Natural Science Foundation of China (NSFC) (Grant Nos. 12074407 and 11774394), the Scientific Instrument Developing Project of the Chinese Academy of Sciences, Grant No. YJKYYQ20190034, Strategic Priority Research Program of Chinese Academy of Sciences (Grant No. XDB33030300), the Key Research Program of Frontier Sciences of Chinese Academy of Sciences (Grant No. QYZDB-SSW-SYS003), Engineering Research Center of Clinical Functional Materials and Diagnosis & Treatment Devices of Zhejiang Province (Grant No: WIUCASK19006), the K. C. Wong Education Foundation. Y. J. thanks Arizona State University for support and Peking University for hospitality during his sabbatical leave.

Conflict of interest

The authors declare no conflict of interest.

Keywords: biological activity · collagen fiber bundles · correlated cell migration · fibrous proteins · long-range force propagation

[1] a) P. Friedl, D. Gilmour, *Nat. Rev. Mol. Cell Biol.* **2009**, *10*, 445 – 457; b) O. Chaudhuri, L. Gu, D. Klumpers, M. Darnell, S. A. Bencherif, J. C. Weaver, N. Huebsch, H. P. Lee, E. Lippens, G. N. Duda, D. J. Mooney, *Nat. Mater.* **2016**, *15*, 326 – 334; c) I. Nitsan, S. Drori, Y. E. Lewis, S. Cohen, S. Tzlil, *Nat. Phys.* **2016**, *12*, 472 – 477; d) M. Huse, *Nat. Rev. Immunol.* **2017**, *17*, 679 – 690; e) J. Wang, F. Lin, Z. Wan, X. Sun, Y. Lu, J. Huang, F. Wang, Y. Zeng, Y. H. Chen, Y. Shi, W. Zheng, Z. Li, C. Xiong, W. Liu, *Sci. Signaling* **2018**, *11*, eaai9192.

[2] a) P. C. Dingal, A. M. Bradshaw, S. Cho, M. Raab, A. Buxboim, J. Swift, D. E. Discher, *Nat. Mater.* **2015**, *14*, 951 – 960; b) W. Xi, T. B. Saw, D. Delacour, C. T. Lim, B. Ladoux, *Nat. Rev. Mater.* **2019**, *4*, 23 – 44; c) C. L. Guo, M. X. Ouyang, J. Y. Yu, J. Maslov, A. Price, C. Y. Shen, *Proc. Natl. Acad. Sci. USA* **2012**, *109*, 5576 – 5582; d) Y. L. Han, P. Ronceray, G. Xu, A. Malandrino, R. D. Kamm, M. Lenz, C. P. Broedersz, M. Guo, *Proc. Natl. Acad. Sci. USA* **2018**, *115*, 4075 – 4080; e) E. Mohagheghian, J. Luo, J. Chen, G. Chaudhary, J. Chen, J. Sun, R. H. Ewoldt, N. Wang, *Nat. Commun.* **2018**, *9*, 1878.

[3] a) C. M. Lo, H. B. Wang, M. Dembo, Y. L. Wang, *Biophys. J.* **2000**, *79*, 144 – 152; b) S. van Helvert, C. Storm, P. Friedl, *Nat. Cell Biol.* **2018**, *20*, 8 – 20; c) A. Shellard, A. Szabó, X. Trepat, R. Mayor, *Science* **2018**, *362*, 339; d) R. Sunyer, V. Conte, J. Escribano, A. Elosegui-Artola, A. Labernadie, L. Valon, D. Navajas, J. M. Garcia-Aznar, J. J. Munoz, P. Roca-Cusachs, X. Trepat, *Science* **2016**, *353*, 1157 – 1161.

[4] J. Irianto, C. R. Pfeifer, Y. Xia, D. E. Discher, *Cell* **2016**, *165*, 1820 – 1820, e1821.

[5] W. J. Han, S. H. Chen, W. Yuan, Q. H. Fan, J. X. Tian, X. C. Wang, L. Q. Chen, X. X. Zhang, W. L. Wei, R. C. Liu, J. L. Qu, Y. Jiao, R. H. Austin, L. Y. Liu, *Proc. Natl. Acad. Sci. USA* **2016**, *113*, 11208 – 11213.

[6] X. Tang, P. Bajaj, R. Bashir, T. A. Saif, *Soft Matter* **2011**, *7*, 6151 – 6158.

[7] a) M. S. Hall, F. Alisafaei, E. Ban, X. Z. Feng, C. Y. Hui, V. B. Shenoy, M. M. Wu, *Proc. Natl. Acad. Sci. USA* **2016**, *113*, 14043 – 14048; b) V. Hakim, P. Silberzan, *Rep. Prog. Phys.* **2017**, *80*, 076601; c) P. H. Wu, A. Giri, S. X. Sun, D. Wirtz, *Proc. Natl. Acad. Sci. USA* **2014**, *111*, 3949 – 3954.

[8] A. D. Doyle, N. Carvajal, A. Jin, K. Matsumoto, K. M. Yamada, *Nat. Commun.* **2015**, *6*, 8720.

[9] S. V. Plotnikov, A. M. Pasapera, B. Sabass, C. M. Waterman, *Cell* **2012**, *151*, 1513 – 1527.

[10] A. S. Piotrowski-Daspit, B. A. Nerger, A. E. Wolf, S. Sundaresan, C. M. Nelson, *Biophys. J.* **2017**, *113*, 702 – 713.

[11] J. I. Puleo, S. S. Parker, M. R. Roman, A. W. Watson, K. R. Eliato, L. Peng, K. Saboda, D. J. Roe, R. Ros, F. B. Gertler, G. Mouneimne, *J. Cell Biol.* **2019**, *218*, 4215 – 4235.

[12] a) S. Nam, K. H. Hu, M. J. Butte, O. Chaudhuri, *Proc. Natl. Acad. Sci. USA* **2016**, *113*, 5492 – 5497; b) F. Pati, J. Gantelius, H. A. Svahn, *Angew. Chem. Int. Ed.* **2016**, *55*, 4650 – 4665; *Angew. Chem.* **2016**, *128*, 4728 – 4743.

[13] a) X. Li, R. Balagam, T. F. He, P. P. Lee, O. A. Igoshin, H. Levine, *Proc. Natl. Acad. Sci. USA* **2017**, *114*, 8974 – 8979; b) X. Ma, M. E. Schickel, M. D. Stevenson, A. L. Sarang-Sieminski, K. J. Gooch, S. N. Ghadiali, R. T. Hart, *Biophys. J.* **2013**, *104*, 1410 – 1418; c) P. Ronceray, C. P. Broedersz, M. Lenz, *Proc. Natl. Acad. Sci. USA* **2016**, *113*, 2827 – 2832; d) H. Nan, Y. Zheng, Y. H. Lin, S. Chen, C. Z. Eddy, J. Tian, W. Xu, B. Sun, Y. Jiao, *Soft Matter* **2019**, *15*, 6938 – 6945; e) R. S. Sopher, H. Tokash, S. Natan, M. Sharabi, O. Shelah, O. Tchaicheeyan, A. Lesman, *Biophys. J.* **2018**, *115*, 1357 – 1370; f) G. K. Xu, B. Li, X. Q. Feng, H. Gao, *Biophys. J.* **2016**, *111*, 1478 – 1486; g) S. He, Y. Green, N. Saeidi, X. Li, J. J. Fredberg, B. Ji, L. M. Pismen, *J. Mech. Phys. Solids* **2020**, *137*, 103860.

[14] a) L. Liang, C. Jones, S. Chen, B. Sun, Y. Jiao, *Phys. Biol.* **2016**, *13*, 066001; b) H. Nan, L. Liang, G. Chen, L. Liu, R. Liu, Y. Jiao, *Phys. Rev. E* **2018**, *97*, 033311; c) Y. Zheng, H. Nan, Y. P. Liu, Q. H. Fan, X. C. Wang, R. C. Liu, L. Y. Liu, F. F. Ye, B. Sun, Y. Jiao, *Phys. Rev. E* **2019**, *100*, 043303.

[15] N. Elkhatib, E. Bresteau, F. Baschieri, A. L. Rioja, G. van Niel, S. Vassilopoulos, G. Montagnac, *Science* **2017**, *356*, eaal4713.

[16] R. Gorelik, A. Gautreau, *Nat. Protoc.* **2014**, *9*, 1931.

[17] C. A. R. Jones, L. Liang, D. Lin, Y. Jiao, B. Sun, *Soft Matter* **2014**, *10*, 8855 – 8863.

[18] A. M. Pasapera, I. C. Schneider, E. Rericha, D. D. Schlaepfer, C. M. Waterman, *J. Cell Biol.* **2010**, *188*, 877 – 890.

[19] a) T. Vicsek, A. Czirók, E. Ben-Jacob, I. Cohen, O. Shochet, *Phys. Rev. Lett.* **1995**, *75*, 1226; b) C. Bechinger, R. Di Leonardo, H. Löwen, C. Reichhardt, G. Volpe, G. Volpe, *Rev. Mod. Phys.* **2016**, *88*, 045006; c) Y. Zheng, Q. Fan, C. Z. Eddy, X. Wang, B. Sun, F. Ye, Y. Jiao, *Phys. Rev. E* **2020**, *102*, 052409.

[20] L. Liu, H. Yu, H. Zhao, Z. Wu, Y. Long, J. Zhang, X. Yan, Z. You, L. Zhou, T. Xia, Y. Shi, B. Xiao, Y. Wang, C. Huang, Y. Du, *Proc. Natl. Acad. Sci. USA* **2020**, *117*, 10832 – 10838.

[21] A. M. Jimenez Valencia, P. H. Wu, O. N. Yogurtcu, P. Rao, J. DiGiacomo, I. Godet, L. J. He, M. H. Lee, D. Gilkes, S. X. Sun, D. Wirtz, *Oncotarget* **2015**, *6*, 43438 – 43451.

Manuscript received: December 2, 2020
Revised manuscript received: January 14, 2021
Accepted manuscript online: February 2, 2020
Version of record online: March 17, 2021

